Novel Compact Mesh Structure Micromixer with Multiple Outlets for Generation of Concentration Gradients

Omar Pandoli[1,2]*, Tommaso Del Rosso[3], Ricardo Queiroz Aucélio[1], Alessandro Massi[4], Chen Xiang[2] and Shu-Ren Hysing[5]

[1]*Department of Chemistry, Universidade Pontificia Catolica, Rio de Janeiro, Brazil*
[2]*Department of Bio-Nano Engineering, Shanghai Jiaotong University, Shanghai, China*
[3]*Department of Physics, Universidade Pontificia Catolica, Rio de Janeiro, Brazil*
[4]*Department of Chemistry, Università di Ferrara, Italy*
[5]*Department of Mathematics, Shanghai Jiaotong University, Shanghai, China*

Received: 31 July 2013; accepted: 11 September 2013

A novel micromixer concept for generation of concentration gradients, inspired by a Chinese design, the traditional Chinese knot "中国结," which features a core mesh structure allowing for a very compact design, is presented. The new concept has been designed using modern computer-aided design (CAD) and computational fluid dynamics (CFD) simulation software and validated by performing multiple experiments. The final design is found to be significantly more compact than conventional ones and allows the use of up to 15 outlet channels.

Keywords: microfluidic, concentration gradient, serial dilution, fluid dynamics, microdevice

In the last decade, many research groups have designed and characterized several microfluidic devices to generate concentration gradients of diffusible samples for different applications and studies in biology (e.g., chemotaxis, cell and enzyme essay) [1], analytical chemistry (e.g., serial dilution of samples) [2], and organic chemistry (e.g., high-throughput parallel synthesis of Au/Ag nanoparticles) [3]. The driving force of this scientific interest is given by the concentration dependence of chemical and biochemical processes and the need to reduce analysis time and waste of expensive raw materials. Until today microreaction technology (MRT) has shown the potential to bypass these problems through developing small, cheap, and stable systems able to generate predictable concentration gradients of the solute with good spatial and temporal control. Recently, Khademhosseini et al. [4] were able to generate stable nonlinear concentration gradients in microfluidic devices for cell studies. They have demonstrated the utility of their microfluidic device to assess the viability of fibroblast cells in response to a range of hydrogen peroxide (H_2O_2).

Whitesides and coworkers [5] previously designed a complex microfluidic network to generate linear concentration gradients; however, the large volume and fast flow rates required to fill up the long mixer channels make it unsuitable to be used with expensive analytes or solvents. Cremer and coworkers [6] have designed and built a simple laminar microfluidic diffusion diluter (μDD) to obtain fixed concentration gradients with different profiles as a function of different and very slow flow rates.

Shinji [7] and Collins [8] were able to create a very interesting but complicated microdevice design to generate diffusion gradient with 8 and 4 channels, respectively.

The goal of this investigation was to create a new compact and simple microfluidic device with up to 15 channels able to create stable nonlinear gradient generation of the reagent solution at relatively high flow rates consuming relatively low amounts of expensive materials.

The design of the laminar microfluidic concentration gradient generator (μCGG) system is illustrated in Figure 1. We got the inspiration for different designs observing Arabic and Chinese geometries; in particular, the Chinese lucky knot had demonstrated the best performance. The main key feature of the μCGG is a compact central grid matrix with a square layout to which it is possible to connect a system of input streams with several outlet streams. The second key feature is the possibility to increase the number of outlets by only slightly increasing the size of the central grid matrix. The complete square grid matrix is formed from single units of smaller squares with a side dimension of 1000 μm. All the inner square units are positioned with their sides parallel to the diagonals of the outer grid square. The inner square units are positioned side by side, and the vertical and parallel channels of the microfluidic channel network with a width of 100 μm are determined.

The input streams are alternated side by side and flow into the channel network by repeatedly dividing and diffusing the streams in different proportions. In this way, an arbitrary number of outlet streams can be created with variable concentration gradient adjusted by means of fine tuning geometrical parameters to vary the fluidic resistance of the channels (see Supporting Information, Figure S1).

Computer-aided design (CAD) tools were used in combination with computational fluid dynamics (CFD) software to design and test many different geometries and channel configurations (Figure 2). The CFD simulations were performed using the COMSOL Multiphysics simulation suite, which is a commercial finite element method-based mathematical modeling and simulation package (see Supporting Information for the theoretical equation model).

Configurations A, B, and C were designed to inject the test solutions via a longer inlet channel system, while configuration D represents a simplified inlet system. In system A, the liquid solution (red and blue) enters into the first channel (n.1), then into the second channel, and so on until the last channel (n.8) has been reached. This inlet system generates a decreasing pressure gradient along the inlet channels. In system B, the liquid solutions are split so that there is equal pressure everywhere before the input solutions enter the core channel system. System C is essentially the opposite of system A and generates an increasing pressure gradient along the inlets. In the last configuration, system D, the two input streams do not have a central main channel to separate the streams and create pressure gradients along with inlet channels, so that the device does not

* Author for correspondence: omarpandoli@puc-rio.br

DOI: 10.1556/JFC-D-13-00021

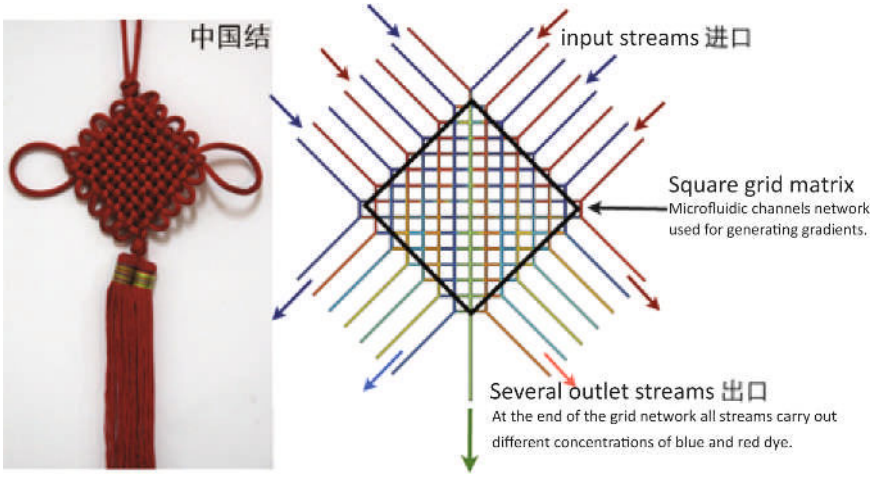

Figure 1. Illustration of the general design concept inspired by a Chinese lucky knot geometry

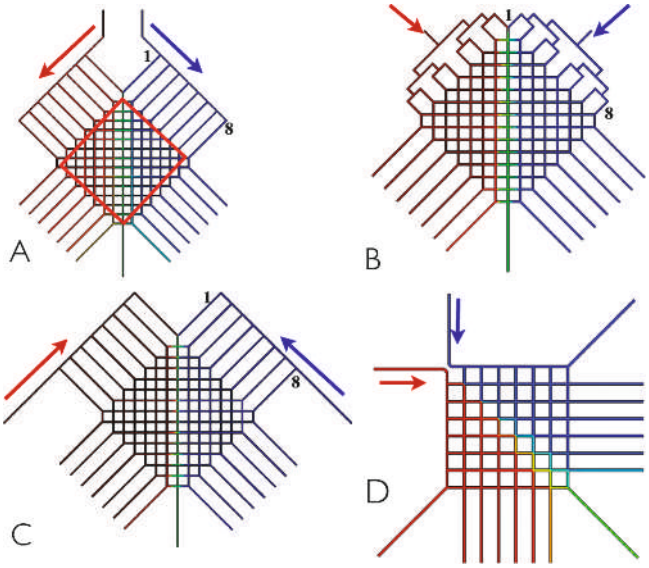

Figure 2. Prototypical micromixer designs (arrows indicate inlets). The grid micromixer concept was initially tested by performing CFD simulations on different geometry designs featuring the same core channel configuration while varying the inlet and outlet configurations

work properly. CFD simulations performed on the different μCGG geometries reveal that the overall best performances in terms of mixing properties and nonlinear gradient concentration at the outlet channels are obtained from system A (Figure 3). From detailed examination of the simulated flow fields, we conclude that a key factor for a successful grid-based micromixing device is that the inlet solutions must flow into a central main channel where a first diffusion mixing can take place. A detailed examination of the phenomena is exposed after. The previous analysis was used to establish a validation design depicted in Figures 3 and 4.

Based on configuration A, we used the relative CAD design to fabricate the new μCGG by soft lithography technique [9] (Figure 4). A master was fabricated in clean room by using contact photolithography and a SU-8 photoresist. The patterns were made on a 4-inch silicon wafer and transferred to poly (dimethylsiloxane) (PDMS) by replica molding. The PDMS replica was cut, and holes for interconnections were made using a needle with an inner diameter of 0.5 mm. The side of the PDMS slab with embossed channels and a glass slide were treated with air plasma cleaner after which the PDMS slab and glass slide were immediately assembled into individual chips. Two PEEK tubes were finally attached as connectors between the syringes and the devices. In Figure 4, water and

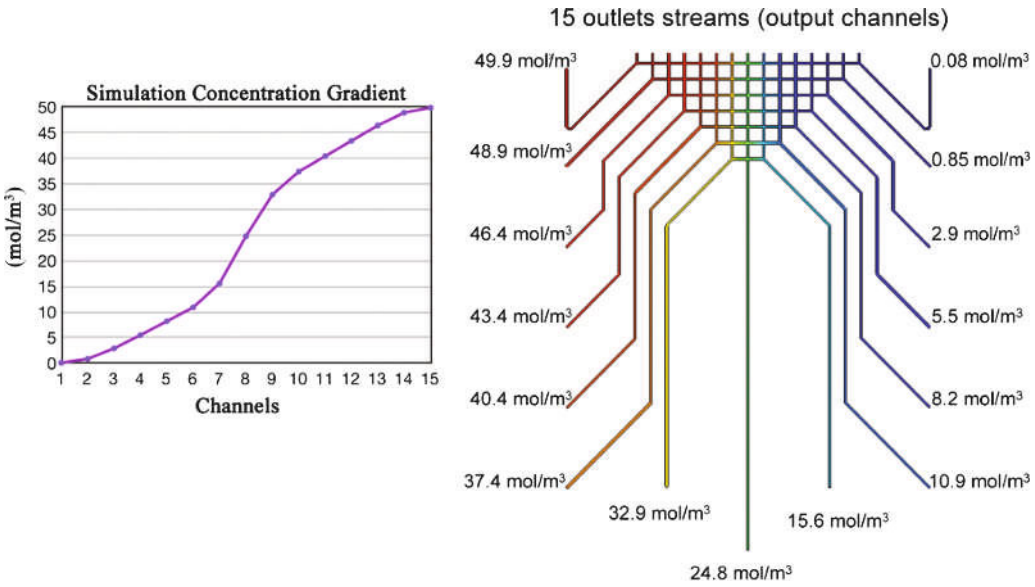

Figure 3. For the design A, the concentration gradient obtained from CFD simulation corresponding to 15 outflow streams is plotted on the left graph. Only one chemical specie (red 50 mol/m^3) is injected using one of the two main inlet channels. The gradient shows a nonlinear (sigmoidal) profile

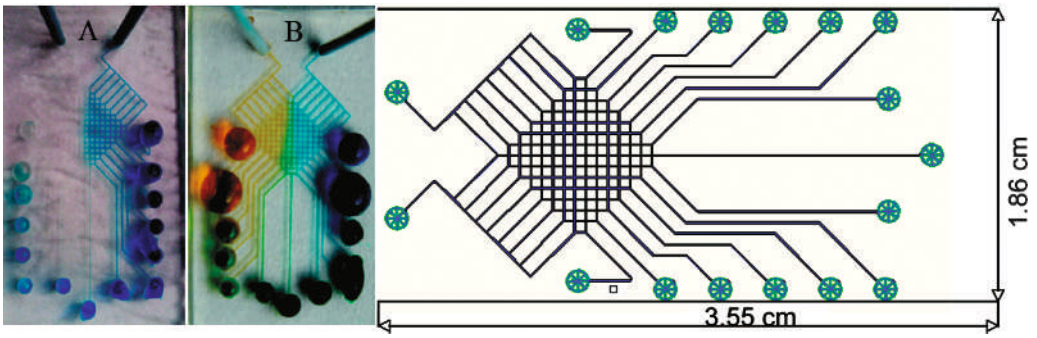

Figure 4. On the left side, the real prototype PDMS on glass (A — with water and blue dye and B — with yellow and blue dyes inlet solutions) is shown, which was realized from the CAD design showed on the right (channel width 100 μm, height 100 μm, central channel)

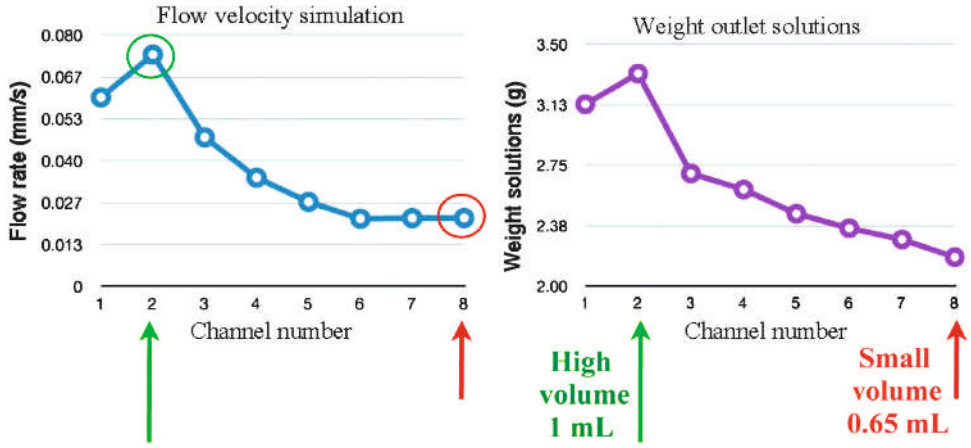

Figure 5. Comparison of simulated data (left) with experimental data of the weighted outflow solutions (right). The CFD data compared well with the measured data, where the flow rate was proportional to the collected weight of the solutions (mm/s) ∝ (g)

different dyes were injected to show that the visible colors change after the mixing inside the grid matrix.

Serial dilution experiments were performed on the μCGG prototype shown in Figure 4, where stream outflow was recollected using PTFE Tubing (PolyTetraFluoroEthylene). The experimental results show that the outflow solution at the longest central channel number 8 was half in volume compared to the solution collected from the second outflow shortest channel (Figure 5).

Since, for a fluid circuit (similar to an electric circuit), the fluidic resistance in the microchannel, R, is proportional to the channel length, the flow rate, Q, will depend on the fluidic resistance R of the channel and the total length of the channel [2].

The simulated results of the flow velocity profile from the μCGG for the first eight channels are shown in the left side of Figure 5; there one can see that the second outflow shortest channel has the largest flow rate, and consequently, the longest central channel (no.8) has the smallest flow rate. In the experiments (right in Figure 5), the shortest channel similarly had the fastest flow rate and the highest collected volume, while the longest channel had the smallest volume. The two profiles are very similar, meaning that the simulated CFD data compared

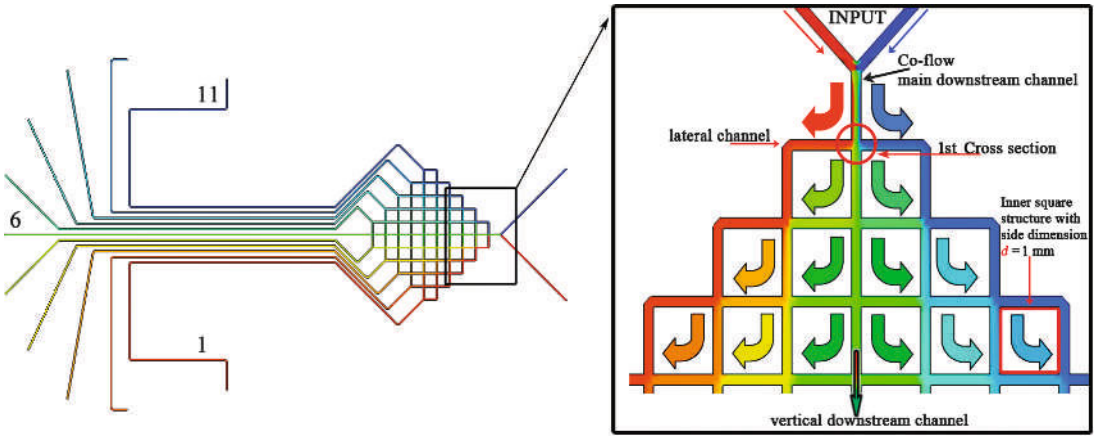

Figure 6. Illustration of the mixing process in a simplified μCGG system with only two inlet channels and 11 outlet streams (zoom on right side). Due to this symmetry and diffusion mixing of the two input streams co-flowing into the main central channel, at each cross, from the first Y junction, different concentrations of the two solutions split off into lateral side channels by diffusive mixing with the vertical downstream solutions. Information dimension: channel width of 100 μm; the main downstream channel n.6 has the shortest length of 30.8 mm from first Y junction; the others have increments of 10% in length

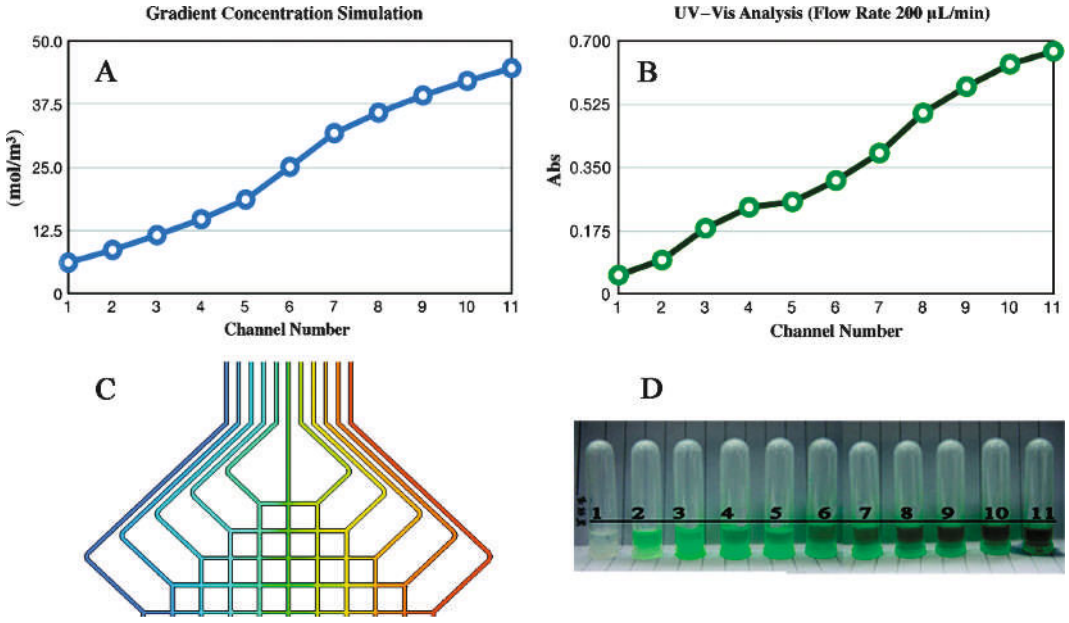

Figure 7. The simulated concentration gradient (A and C) was validated using a UV–vis spectrophotometric analysis (B and D)

very well with the experimental data. These preliminary results allowed us to trust the modeling and simulation approach and utilize it to improve the performance of the micromixer and realize an optimized design.

An additional optimization of the design and reconfiguration of the inlet system and outflow cannels were subsequently carried out (Figure 6). The inlet system was simplified with a unique mix point before entering to the central square grid matrix. Moreover the outlet streams were reduced up to 11 channels. From detailed examination of the simulated flow fields for the simplified design, we confirmed that a key ingredient to a successful grid-based micromixing device is that the input solutions must flow into a main channel where a diffusion mixing can take place before splitting out into the lateral channels. This concept is illustrated in Figure 6 (zoom on the right) for mixing of red and blue dye. Along the vertical main downstream channel, diffusive mixing between the two solutions creates a concentration gradient of co-flowing solutions, and at every cross section from the two sides, different concentrations of the solutions can be split off to the horizontal channels. When the solutions enter into a new horizontal channel, the concentration can again be changed by mixing with the downward flowing vertical streams.

For the final validation of the simulated concentration data, we tested the performance of the simplified µCGG system by carrying out an ultraviolet–visible (UV–vis) spectrophotometric analysis for the recollected output stream solutions at a flow rate of 200 µL/min. The maximum absorption at 408 nm for the green solutions is plotted in Figure 7B where a gradient generation with a sigmoidal profile can be observed. This matches very well to the concentration gradient profile generated by the CFD simulation (Figure 7A). Other UV–vis analysis shown in Supporting Information was performed with different flow rate from 10 to 50 µL/min (see ESM, Figure S2).

Due to the compact nature of the µCGG system, the inherently shorter inlet channels make the outputs more susceptible to variations of pressure. To avoid this disadvantage of the mixer, we increased the channel length of the two inlet channels before injecting into the Y junction; this is able to stabilize the flow perturbation into the micromixer.

In conclusion, a novel two-dimensional concentration gradient generator (CGG) has been designed and tested by a combination of CAD design, CFD simulations, and experimental techniques. The combination of mathematical modeling, CAD and CFD simulations in the prototyping stage, enabled a very quick and efficient virtual concept testing. In this way, the actual manufacturing stage only had to take place as a very last step when the modeling approaches all agreed on the design, thus, maximizing the probability that the design is working and efficient. Compared with an experimental approach, trial-and-error, the time and costs for experimental testing, redesign, and remanufacturing were thus significantly reduced. The most time consuming part in the modeling and simulation process was to draw the different micromixing designs in an external CAD tool. After the CAD designs were imported into COMSOL, the simulation and analysis process was quite straightforward and efficient. The results from the simulations could directly be postprocessed in the same software to see the degree of mixing at the outlets and pressure drop over the mixing device, as well as examine in detail the local flow field in the microchannels.

The resulting µCGG system, for which the CFD data closely follow the experimental data, is significantly smaller than the present state of the art, and the grid design allows for up to 15 outflow channels in a very compact package. The compact design also reduces the waste of expensive material. The generation of different concentration profiles can also be adjusted by fine tuning geometrical and operating parameters so as to vary the fluidic resistance of the channels. A suitable topology of the device can also be chosen according to a user prescribed concentration profile (e.g., linear or parabolic shaped).

We believe that the concentration generation gradient system herein described might be useful for a wide range of applications based on nanosynthesis, thanks to the easy modulation of the molar ratio between the reagents in the feed solutions at relatively high flow rates (10–300 µL/min). The optimization by this approach of synthetically relevant photoreductions is currently underway in our laboratories as well as the utilization of the µCGG system for the rapid evaluation of the kinetics of model reactions. More complex designs are also under study to further improve the performance of the disclosed microfluidic device, and our progress will be reported in due course.

Acknowledgement. We gratefully acknowledge the European Commission through the Science and Technology Fellowship Program in China (EuropeAid/127024/L/ACT/CN), for funding the research and the fellowship of O.P. and S.R.H. This work was supported also by China Postdoctoral Science Foundation

(20100470687) and the Agency FAPERJ (E-26/111.848/2012 and E-26/112.096/2012). Preliminary results of this work were presented at the 2nd Asia-Pacific Chemical and Biological Microfluidics Conference (APCBM 2011) in Nanjing, China.

Supporting Information

Electronic Supplementary Material (ESM) is available on mathematical modeling and simulation in the online version at: doi:10.1556/JFC-D-13-00021.

References

1. (a) O'Neill, A. T.; Monteiro-Riviere, N.; Walker, G. M. *Conf. Proc. IEEE Eng. Med. Biol. Soc.* **2006**, *1*, 2836–2839; (b) Cimetta, E.; Cannizzaro, C.; James, C.; Biechele, T.; Nicola Elvassore, N.; Vunjak-Novakovic, G. *Lab Chip* **2010**, *10*, 3277–3283; (c) Wu, M. H.; Huang, S. B.; Lee, G. B. *Lab Chip* **2010**, *8*, 939–956; (d) Upadhaya, S.; Selvaganapathy, P. R. *Crit. Rev. Biomed. Eng.* **2009**, *3*, 193–257; (e) Chia-Hsien, Y.; Chien-Hsien, C.; Yu-Cheng, L. *Microfluid. Nanofluid.* **2011**, *10*, 1011–1018.

2. (a) Choong, K.; Kangsun, L.; Jong, H. K.; Kyeong, S. S.; Kyu-Jung, L.; Tae Song, K.; Ji, Y. K. *Lab Chip* **2008**, *8*, 473–479; (b) Dertinger, S. K. W.; Chiu, D. C.; Jeon, N. L.; M. Whitesides, G. M. *Anal. Chem.* **2001**, *73*, 1240–1246.

3. Yang, C. G.; Xu, Z. R.; Lee, A. P.; Wang, J. H. *Lab Chip* **2013**, *13*, 2815–2820.

4. Khademhosseini, A.; Selimovi, S.; Sim, W. Y.; Kim, S. B.; Jang, Y. H.; Lee, W. G. *Anal. Chem.* **2011**, *83*, 2020–2028.

5. Whitesides, G. M.; Jeon, N. L.; Dertinger, S. K.; Chiu, D. T.; Choi, I. S.; Stroock, A. D. *Langmuir* **2000**, *16*, 8311–8316.

6. Cremer, P. S.; Holden, M. A.; Kumar, S.; Castellana, E. T.; Beskok, A. *Sens. Actuators, B* **2003**, *92*, 199–207.

7. Koji, H.; Shinji, S.; Toshiyuki, K. *Lab Chip* **2009**, *9*, 1763–1772.

8. Smith, R. L.; Demers, C. J.; Collins, S. D. *Microfluid. Nanofluid.* **2010**, *9*, 613–622.

9. Duffy, D. C.; McDonald, J. C.; Schueller, O. J. A.; Whitesides, G. M. *Anal. Chem.* **1998**, *70*, 4974–4984.